Strong-coupling spectrum in the Hamiltonian limit of the SU(2) Wilson action in 2+1 dimensions

1 Monte Carlo simulations

Results are presented in Tables 1-8 for the energies, multiplied by ξa_s, for the glue in the presence of a static quark and antiquark separated by R lattice spacings along an axis of the lattice. Simulations were done using the anisotropic $2+1$-dimensional Wilson SU(2) gauge-field action (without tadpole improved couplings) at strong coupling $\beta = 1/2$. Results are from simulations on an $8^2 \times 320$ lattice, while the results for $\xi \to \infty$ were obtained by extrapolating the results linearly in $1/\xi$. The rows labeled by SC indicate the results from strong coupling perturbation theory. Note that a_s and a_t are the spatial and temporal lattice spacings, respectively, and ξ is the aspect ratio a_s/a_t. States labeled by S and A are symmetric and antisymmetric, respectively, under reflections in the molecular axis. States with a subscript g and u are symmetric and antisymmetric, respectively, under the combined operations of charge conjugation and spatial inversion about the midpoint between the quark and the antiquark. The strong-coupling perturbation theory results were done in the Hamiltonian formulation. The transfer-matrix method is needed to determine the relationship between our simulation results and the spectrum obtained in the Hamiltonian approach[1]. The transfer matrix T is related to the Hamiltonian H by

$$T = C \exp\left[-a_t H + O(a_t^2)\right]. \tag{1}$$

2 Strong-coupling perturbation theory

We begin by replacing space (but not time) by a discrete cubic lattice with spacing a. The gauge field is defined on the links connecting the sites of the lattice. Each directed link may be occupied by a bit of chromoelectric flux, similar to a dipole with coloured ends. The coloured ends are described by a representation of $SU(N)$ colour. The colour content of the two ends are not independent. If one end is in the R representation, then the other end must be in the complex conjugate representation $\overline{R}$. The link can be pictured as a line of chromoelectric flux whose terminals transform as a particle-antiparticle pair. We shall describe this situation by saying that the link (x, i) starting at site x and extending in the direction i is in the state $(R, \overline{R})$. However, this does not completely specify the state of the link. We must also specify the directions of the colours in the representation space. Thus, the link is completely specified by a vector V_{ab} where a and b transform as indices in the $(R, \overline{R})$ representation of $SU(N) \times SU(N)$.

The most elementary flux is the one in the fundamental $(N, \overline{N})$ or $(\overline{N}, N)$ representation. From such elementary fluxes, all others can be constructed in the same way that all irreducible representations of $SU(N)$ can be built out of N and $\overline{N}$. Let us introduce a flux operator $U_{jk}(x, i)$. The index j is associated with the flux end at x and acts in the fundamental N representation. The index k is associated with the other end at $x + a\hat{i}$ and acts in

Table 1: Results for $R = 3$ in the S_g channel.

ξ	S_g	S'_g	S''_g	S'''_g	S''''_g
25	9.3609(11)	15.3377(33)	15.6145(35)	15.6222(30)	15.8982(38)
40	9.22344(60)	15.1036(24)	15.3849(22)	15.3894(15)	15.6698(24)
55	9.1607(13)	15.0030(47)	15.2800(28)	15.2842(30)	15.5637(51)
∞	8.9941(19)	14.7183(67)	15.0016(55)	15.0019(51)	15.2873(73)
SC	8.99554	14.72049	15.00000	15.00000	15.27951

Table 2: Results for $R = 3$ in the A_u channel.

ξ	A_u	A'_u	A''_u	A'''_u
25	15.3360(30)	15.6172(33)	15.6190(35)	15.8972(35)
40	15.1032(24)	15.3812(16)	15.3863(19)	15.6654(23)
55	14.9991(43)	15.2788(35)	15.2839(45)	15.5617(55)
∞	14.7168(63)	14.9922(56)	15.0011(65)	15.2800(72)
SC	14.72049	15.00000	15.00000	15.27951

Table 3: Results for $R = 3$ in the A_g and S_u channels.

ξ	A_g	A'_g	S_u	S'_u
25	15.4935(33)	15.7387(25)	15.4914(24)	15.7400(28)
40	15.2582(16)	15.5115(20)	15.2612(20)	15.5155(18)
55	15.1519(36)	15.4058(40)	15.1555(33)	15.4037(39)
∞	14.8666(57)	15.1309(55)	14.8764(50)	15.1335(55)
SC	14.87500	15.12500	14.87500	15.12500

Table 4: Results for $R = 4$.

ξ	S_g	S'_g	S''_g	S'''_g	S''''_g
25	12.4813(16)	18.3963(45)	18.6205(35)	18.6480(40)	18.8300(35)
40	12.29884(96)	18.1177(30)	18.3389(20)	18.3711(23)	18.5585(26)
55	12.2148(17)	17.9944(55)	18.2117(39)	18.2455(48)	18.4284(47)
∞	11.9936(28)	17.6566(86)	17.8703(63)	17.9098(74)	18.1000(70)
SC	11.99405	17.65849	17.87500	17.90849	18.09151

Table 5: Results for $R = 4$.

ξ	$S_g^{(v)}$	$S_g^{(vi)}$	A_u	A'_u
25	18.8712(35)	19.0835(48)	18.3940(40)	18.6160(35)
40	18.5945(23)	18.8083(28)	18.1158(29)	18.3373(24)
55	18.4663(55)	18.6813(72)	17.9872(61)	18.2161(45)
∞	18.1315(72)	18.3483(93)	17.6504(84)	17.8777(68)
SC	18.12500	18.34151	17.65849	17.87500

Table 6: Results for $R = 4$.

ξ	A''_u	A'''_u	A''''_u	$A_u^{(v)}$
25	18.6515(30)	18.8287(33)	18.8678(38)	19.0797(50)
40	18.3668(21)	18.5524(23)	18.5865(24)	18.8029(33)
55	18.2384(45)	18.4263(47)	18.4650(54)	18.6796(55)
∞	17.8930(62)	18.0915(66)	18.1226(75)	18.3442(91)
SC	17.90849	18.09151	18.12500	18.34151

Table 7: Results for $R = 4$.

ξ	A_g	A'_g	A''_g	A'''_g
25	18.5220(35)	18.7368(40)	18.7377(38)	18.9542(35)
40	18.2433(22)	18.4561(22)	18.4609(21)	18.6797(25)
55	18.1174(46)	18.3353(52)	18.3374(41)	18.5524(45)
∞	17.7795(67)	17.9935(74)	18.0018(66)	18.2198(69)
SC	17.78349	18.00000	18.00000	18.21651

Table 8: Results for $R = 4$.

ξ	S_u	S'_u	S''_u	S'''_u
25	18.5212(40)	18.7347(48)	18.7410(35)	18.9530(33)
40	18.2450(20)	18.4584(24)	18.4646(18)	18.6835(20)
55	18.1179(47)	18.3324(45)	18.3399(39)	18.5534(51)
∞	17.7832(71)	17.9973(78)	18.0048(61)	18.2295(65)
SC	17.78349	18.00000	18.00000	18.21651

the complex conjugate representation $\overline{N}$. Finally, U_{jk} must be a unitary matrix. Note that $U_{ij}(x,k)$ and $U_{ij}(x+a\hat{k},-k)$ are not independent since they describe the same undirected link. In fact, $U(x+a\hat{k},-k) = U^\dagger(x,k) = U^{-1}(x,k)$.

The simplest state of a link is the one in which the flux is absent. We say in this case that the flux is in the singlet representation. We shall denote this state by $|0\rangle$ and require unit normalization. A state of elementary flux is created by applying $U(x,k)$ to $|0\rangle$. Higher dimensional representations are obtained by applying the U operator repeatedly. A complete basis of states can be generated by applying the U to $|0\rangle$. Note that we can consider the matrix representations of U in higher representations. In such cases, we denote the operator by $U^{(R)}$. When the superscript is absent, the fundamental representation is to be assumed. Note that $U^{(R)}_{ab} \neq U^{(\overline{R})}_{ab} = U^{(R)\dagger}_{ba}$. We shall label the (unit normalized) basis states of a given link (x,i) by $|(x,i);R;ab\rangle$. We find that

$$|(x,i);R;ab\rangle = \sqrt{d_R}\, U^{(R)}_{ab}(x,i)\ |0\rangle, \tag{2}$$

where d_R is the dimension of the R representation. The main tool in constructing these states is the Clebsch-Gordan series:

$$U^{(R_1)}_{AB} U^{(R_2)}_{ab} = \sum_{R,\alpha,\beta} \langle R_1, A; R_2, a|R,\alpha\rangle\ U^{(R)}_{\alpha\beta}\ \langle R,\beta|R_1,B;R_2,b\rangle. \tag{3}$$

The Clebsch-Gordan coefficients satisfy

$$\sum_{\alpha_1,\alpha_2} \langle R,\alpha|R_1,\alpha_1;R_2,\alpha_2\rangle\langle R_1,\alpha_1;R_2,\alpha_2|R,\beta\rangle = \delta_{\alpha\beta} \qquad \text{if } R \text{ appears in } R_1\otimes R_2. \tag{4}$$

Also, note the important relation:

$$\langle 0|U^{(R)}_{\alpha\beta}|0\rangle = \delta_{R1}, \tag{5}$$

which is nonzero only when R is the identity representation.

As examples of the Clebsch-Gordan coefficients, we have the following in $SU(2)$:

$$\begin{aligned}
\langle 2a;\overline{2}b|1\rangle &= \langle \overline{2}a;2b|1\rangle = \sqrt{\tfrac{1}{2}}\ \delta_{ab}, && (6)\\
\langle 2a;2b|1\rangle &= \langle \overline{2}a;\overline{2}b|1\rangle = \sqrt{\tfrac{1}{2}}\ \epsilon_{ba}, && (7)\\
\langle 2a,\overline{2}b|3k\rangle &= \sqrt{\tfrac{1}{2}}\ (\sigma_k)_{ab}, && (8)\\
\langle \overline{2}a,2b|3k\rangle &= \sqrt{\tfrac{1}{2}}\ (\sigma_k)_{ba}, && (9)\\
\langle 3a;3b|3k\rangle &= \sqrt{\tfrac{1}{2}}\ \epsilon_{kab}, && (10)\\
\langle 2a;2b|3k\rangle &= \sqrt{\tfrac{1}{2}}\ (\sigma_k)_{bc}\epsilon_{ca}, && (11)\\
\langle \overline{2}a;\overline{2}b|3k\rangle &= \sqrt{\tfrac{1}{2}}\ \epsilon_{bc}(\sigma_k)_{ca}, && (12)
\end{aligned}$$

where σ_k denotes the standard Hermitian Pauli spin matrices and ϵ_{ab} and ϵ_{abc} are the fully antisymmetric Levi-Civita tensors on 2 and 3 indices, respectively, with $\epsilon_{12} = 1$ and $\epsilon_{123} = 1$.

Note that we must proceed with some care in $SU(2)$ since the $\overline{2}$ representation is equivalent to the fundamental 2 representation:

$$U^{(\overline{2})}_{ab} = U^{\dagger}_{ba} = \epsilon_{aa'} U_{a'b'} \epsilon_{bb'}. \tag{13}$$

Hence,

$$\begin{aligned} U_{ij}\ U^{\dagger}_{kl} &= \tfrac{1}{2}\delta_{il}\delta_{kj} + \tfrac{1}{2}\sigma^a_{il}\ \sigma^b_{kj}\ U^{(3)}_{ab}, & (14)\\ U_{ij}\ U_{kl} &= \tfrac{1}{2}\epsilon_{ki}\epsilon_{lj} - \tfrac{1}{2}\sigma^a_{km}\epsilon_{mi}\epsilon_{jn}\sigma^b_{nl}\ U^{(3)}_{ab}. & (15)\end{aligned}$$

Note that $(\sigma_k)_{il}\epsilon_{lj} = (\sigma_k)_{jl}\epsilon_{li}$.

On a given link, the space of states spanned by $|R;ab\rangle$ for fixed R is a d_R^2 dimensional subspace. The projection operator onto this subspace is denoted P_R and is given by

$$\begin{aligned} P_R &= \sum_{ab} |R;ab\rangle\langle R;ab|, \\ &= d_R \sum_{ab} U^{(R)}_{ab}|0\rangle\langle 0|U^{(R)\dagger}_{ba}. & (16)\end{aligned}$$

Using Eqs. 5 and 14 we can easily show that

$$\begin{aligned} \langle 0|U^{\dagger}_{ij}P_2 U_{kl}|0\rangle &= \tfrac{1}{2}\delta_{il}\delta_{jk}, & (17)\\ \langle 0|U^{\dagger}_{ij}U_{kl}P_1 U^{\dagger}_{rs}U_{tu}|0\rangle &= \tfrac{1}{4}\delta_{il}\delta_{jk}\delta_{ru}\delta_{st}, & (18)\\ \langle 0|U^{\dagger}_{ij}U_{kl}P_3 U^{\dagger}_{rs}U_{tu}|0\rangle &= \tfrac{1}{12}\left(2\delta_{ks}\delta_{jt} - \delta_{jk}\delta_{st}\right)\left(2\delta_{iu}\delta_{lr} - \delta_{il}\delta_{ru}\right). & (19)\end{aligned}$$

In $SU(3)$, we have

$$\begin{aligned} \langle 1|3i;\overline{3}j\rangle &= \sqrt{\tfrac{1}{3}}\ \delta_{ij}, & (20)\\ \langle 8,\alpha|3i,\overline{3}j\rangle &= \sqrt{\tfrac{1}{2}}\ \lambda^{\alpha}_{ij}, & (21)\\ \langle \overline{3}i|3j;3k\rangle &= \sqrt{\tfrac{1}{2}}\ \epsilon_{ijk}, & (22)\\ \langle 6\{kl\}|3i;3j\rangle &= \tfrac{1}{2}\ (\delta_{ik}\delta_{jl} + \delta_{il}\delta_{jk}), & (23)\end{aligned}$$

where λ^a are the standard Gell-Mann matrices. Note that

$$\sum_a \sigma^a_{ij}\ \sigma^a_{kl} = 2\ \delta_{il}\delta_{jk} - \delta_{ij}\delta_{kl}, \tag{24}$$

$$\sum_a \lambda^a_{ij}\ \lambda^a_{kl} = 2\ \delta_{il}\delta_{jk} - \tfrac{2}{3}\ \delta_{ij}\delta_{kl}. \tag{25}$$

The complete set of states for the lattice is the tensor product formed from the space of states of each link. However, not every state in this space of states is physically allowed. The allowable states are those which are locally gauge invariant.

The Wilson gluon Hamiltonian on a spatial lattice (time is continuous) is given by

$$H_{\rm glue} = \frac{g^2}{2a}\sum_{la} E^a_l E^a_l + \frac{1}{ag^2}\sum_p {\rm Tr}(2 - U_p - U_p^{\dagger}), \tag{26}$$

where l refers to the links of the lattice, and p refers to the plaquettes of the lattice, and U_p means the product of the four link variables around the plaquette p. E_l^a is essentially the conjugate momentum to U_l, satisfying the equal-time commutation relation

$$[E_l^a, U_{l'}] = \delta_{ll'}\ U_l\ T^a, \tag{27}$$

where $T^a = \sigma^a/2$ in $SU(2)$ and $T^a = \lambda^a/2$ in $SU(3)$. The strong-coupling eigenstates are the eigenvectors of $\sum_l E_l^a E_l^a$. For our strong-coupling perturbation theory calculations, discard the irrelevant constant in $H_{\rm glue}$ and define

$$\frac{2a}{g^2}H = H_0 - xH_{\rm int}, \tag{28}$$

$$H_0 = \sum_l E_l^a E_l^a, \tag{29}$$

$$H_{\rm int} = \frac{1}{2}\sum_p {\rm Tr}\left(U_p + U_p^\dagger\right), \tag{30}$$

where $x = 4/g^4$ is the small expansion parameter. Now in $SU(2)$, ${\rm Tr}U_p = {\rm Tr}U_p^\dagger$ which simplifies $H_{\rm int}$ slightly.

Our goal is to determine the spectrum of $SU(2)$ glue in the presence of a static quark-antiquark pair in 2+1 dimensions. The first step is to determine the energy of the vacuum state (without the quark-antiquark) as a function of x. At zero-th order, the vacuum state is simply $|0\rangle$, the state in which all links are in their ground state. Since $H_0|0\rangle = 0$, $\mathcal{E}_{\rm vac}^{(0)} = 0$. At first order in perturbation theory,

$$\mathcal{E}_{\rm vac}^{(1)} = -x\langle 0|H_{\rm int}|0\rangle = 0. \tag{31}$$

At second order in perturbation theory,

$$\mathcal{E}_{\rm vac}^{(2)} = x^2 \sum_{m\neq 0} \frac{|\langle m|H_{\rm int}|0\rangle|^2}{\mathcal{E}_0^{(0)} - \mathcal{E}_m^{(0)}}. \tag{32}$$

The strong-coupling states $|m\rangle$ which contribute to this sum are those in which the links of a single plaquette have been excited to their first-excited state and combined in a gauge-invariant manner. There are $N_{\rm plaq}$ such states, where $N_{\rm plaq}$ is the number of plaquettes in the lattice. Each state has the same energy: $\mathcal{E}_m^{(0)} = 4C_F = 4(3/4) = 3$, where $C_F = (N^2-1)/(2N)$ is the quadratic Casimir in $SU(N)$. So to evaluate $\mathcal{E}_{\rm vac}^{(2)}$, we can concentrate on a single plaquette, as shown below.

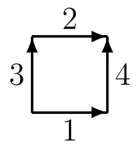

The normalized state $|m\rangle$ is

$${\rm Tr}[U(3)U(2)U^\dagger(4)U^\dagger(1)]\ |0\rangle. \tag{33}$$

To check the normalization, we use Eqs. 5 and 14 as follows:

$$\begin{aligned}
& \langle 0|\ \mathrm{Tr}[U(3)U(2)U^\dagger(4)U^\dagger(1)]\ \mathrm{Tr}[U(1)U(4)U^\dagger(2)U^\dagger(3)]\ |0\rangle \\
= & \langle 0|\ U_{ab}(3)U_{bc}(2)U^\dagger_{cd}(4)U^\dagger_{da}(1)U_{ij}(1)U_{jk}(4)U^\dagger_{kl}(2)U^\dagger_{li}(3)\ |0\rangle, \\
= & \frac{1}{2}\delta_{ai}\delta_{dj}\ \frac{1}{2}\delta_{ck}\delta_{bl}\ \frac{1}{2}\delta_{ai}\delta_{bl}\ \frac{1}{2}\delta_{ck}\delta_{dj}, \\
= & \frac{1}{16}\delta_{ii}\delta_{jj}\delta_{kk}\delta_{ll}, \\
= & 1.
\end{aligned} \tag{34}$$

Hence, substituting in $H_{\rm int}$, we find

$$\begin{aligned}
\mathcal{E}^{(2)}_{\rm vac} &= -\frac{x^2}{3}N_{\rm plaq}\left|\langle 0|\ \mathrm{Tr}[U(3)U(2)U^\dagger(4)U^\dagger(1)]\ \mathrm{Tr}[U(1)U(4)U^\dagger(2)U^\dagger(3)]\ |0\rangle\right|^2 \\
&= -\frac{x^2}{3}N_{\rm plaq}.
\end{aligned} \tag{35}$$

To summarize,

$$\mathcal{E}_{\rm vac} = -\frac{x^2}{3}N_{\rm plaq}. \tag{36}$$

Now place a static quark and antiquark on the lattice, separated by a distance La along an axis of the lattice. Since the quark and antiquark are static, we need not worry about their spins or their fermionic nature; they can be treated simply as colour sources. We now wish to find the energy of the lowest-lying stationary state of the glue in the presence of this pair. At zero-th order in perturbation theory, the lowest-lying state is one in which the L links connecting the quark and the antiquark have been excited into their first-excited state, while all other links are in their ground state. Hence,

$$\mathcal{E}^{(0)}_{\overline{Q}Q} - \mathcal{E}^{(0)}_{\rm vac} = C_F L = \frac{3}{4}L. \tag{37}$$

We shall denote this state by $|\Omega_L\rangle$. Once again, the contribution at first-order in perturbation theory is again zero. The second-order contribution requires a little bit of work. The intermediate states which contribute at second order can be divided up into the following classes, as shown in Table 9: (a) those in which a single plaquette, disconnected from the line connecting the quark and the antiquark, is excited into the fundamental representation; (b) those in which $L-1$ of the links connecting the quark and antiquark are in the fundamental representation, while the one remaining link along the molecular axis (in the p-th position) is in its ground state and the three links which form a staple around the p-th link are all in the fundamental representation; (c) those similar to (b), except that the p-th link is in the adjoint representation; (d) those in which $L+4$ links are excited into the fundamental representation as shown in Table 9.

Each intermediate state in class (a) contributes the same as it would in the vacuum: $-x^2/3$.

To determine the contribution from diagrams in class (b), it suffices to examine the case for a specific L, say $L=3$. We first label the links as shown below:

Table 9: Contributions to $\mathcal{E}_{\overline{Q}Q}$ from various classes of diagrams at second-order in perturbation theory. Lattice sites are indicated by the dots. Links in the fundamental representation are indicated by simple line segments connecting neighbouring sites. Links in the adjoint representation are depicted by a line segment with an open circle connecting neighbouring sites. All other links are in their ground states. $\mathcal{E}^{(2)}_{\overline{Q}Q}$ is obtained by multiplying each contribution by the corresponding multiplicity, summing the results, then multiplying by x^2.

	Multiplicity	Intermediate state	Contribution
(a)	$N_{\text{plaq}} - 2L - 4$	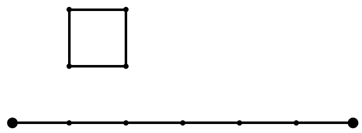	$-\frac{1}{3}$
(b)	$2L$	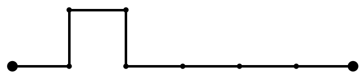	$-\frac{1}{6}$
(c)	$2L$	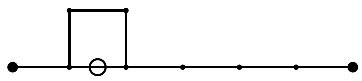	$-\frac{3}{14}$
(d)	4	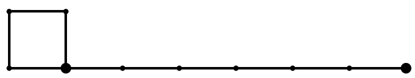	$-\frac{1}{3}$

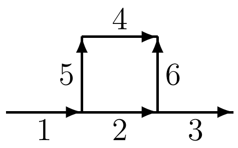

The normalized starting and intermediate states are (ignoring the colour sources):

$$|\Omega_{3;\alpha\beta}\rangle = \sqrt{2}\,[U(1)U(2)U(3)]_{\alpha\beta}\,|0\rangle, \tag{38}$$
$$|b_{\alpha\beta}\rangle = \sqrt{2}\left[U(1)U(5)U(4)U^\dagger(6)U(3)\right]_{\alpha\beta}|0\rangle. \tag{39}$$

Now

$$H_0|\Omega_{3;\alpha\beta}\rangle = \frac{3}{4}L\ |\Omega_{3;\alpha\beta}\rangle, \tag{40}$$
$$H_0|b_{\alpha\beta}\rangle = \frac{3}{4}(L+2)\ |b_{\alpha\beta}\rangle, \tag{41}$$

and

$$\begin{aligned}\langle b_{rs}|H_{\rm int}|\Omega_{3;\alpha\beta}\rangle &= 2\langle 0|\left[U^\dagger(3)U(6)U^\dagger(4)U^\dagger(5)U^\dagger(1)\right]_{sr}\\ &\quad\times{\rm Tr}\left[U(5)U(4)U^\dagger(6)U^\dagger(2)\right][U(1)U(2)U(3)]_{\alpha\beta}|0\rangle,\\ &= 2\langle 0|U^\dagger_{st}(3)U_{tu}(6)U^\dagger_{uv}(4)U^\dagger_{vw}(5)U^\dagger_{wr}(1)\\ &\quad\times U_{ij}(5)U_{jk}(4)U^\dagger_{kl}(6)U^\dagger_{li}(2)U_{\alpha\mu}(1)U_{\mu\nu}(2)U_{\nu\beta}(3)|0\rangle,\\ &= 2\ \tfrac{1}{2}\delta_{w\mu}\delta_{\alpha r}\ \tfrac{1}{2}\delta_{l\nu}\delta_{i\mu}\ \tfrac{1}{2}\delta_{s\beta}\delta_{t\nu}\ \tfrac{1}{2}\delta_{uk}\delta_{vj}\ \tfrac{1}{2}\delta_{vj}\delta_{wi}\ \tfrac{1}{2}\delta_{tl}\delta_{uk},\\ &= \tfrac{1}{2}\delta_{\alpha r}\delta_{s\beta}.\end{aligned} \tag{42}$$

Then

$$\sum_{rs}|\langle b_{rs}|H_{\rm int}|\Omega_{3;\alpha\beta}\rangle|^2 = \frac{1}{4}\sum_{rs}\delta_{\alpha r}\delta_{s\beta}\delta_{\alpha r}\delta_{s\beta} = \frac{1}{4}, \tag{43}$$

and the contribution to the energy is $-x^2/6$.

We can now repeat the above steps for the diagrams in class (c). First, we find

$$H_0|c_{\alpha\beta}\rangle = \left[\frac{3}{4}(L+2)+2\right]\ |c_{\alpha\beta}\rangle, \tag{44}$$

since the quadratic Casimir for the adjoint representation is $C_A = N$ in $SU(N)$. Next, we need to determine the intermediate state. This requires some Clebsch-Gordanry to ensure a gauge-invariant state. However, we can circumvent this by noting that since our starting state is gauge-invariant and $H_{\rm int}$ is gauge-invariant, then matrix elements with intermediate states which are not gauge-invariant will vanish. Hence, we can sum over all intermediate states, not just the physical intermediate states. This then eliminates the need to determine how the colour indices are matched at the lattice sites in the intermediate states. In other words, we can proceed using link projectors. Let $P_R(l)$ denote the projection operator into the irreducible representation R associated with link l. This operator is given by

$$P_R(l) = \sum_{\alpha\beta}|l;R;\alpha\beta\rangle\langle l;R;\alpha\beta|, \tag{45}$$
$$= d_R\sum_{\alpha\beta}U^{(R)}_{\alpha\beta}(l)|0\rangle\ \langle 0|U^{(R)\dagger}_{\beta\alpha}(l). \tag{46}$$

Then, using Eqs. 17 and 19,

$$
\begin{aligned}
\sum_{rs} |\langle c_{rs}|H_{\rm int}|\Omega_{3;\alpha\beta}\rangle|^2 &= \langle\Omega_{3;\alpha\beta}|\ H_{\rm int}\ P_2(1)P_3(2)P_2(3)P_2(5)P_2(4)P_2(6)\ H_{\rm int}\ |\Omega_{3;\alpha'\beta'}\rangle, \\
&= 2\langle 0|\left[U^\dagger(3)U^\dagger(2)U^\dagger(1)\right]_{\beta\alpha}\ {\rm Tr}\left[U(2)U(6)U^\dagger(4)U^\dagger(5)\right] \\
&\quad \times P_2(1)P_3(2)P_2(3)P_2(5)P_2(4)P_2(6)\ {\rm Tr}\left[U(5)U(4)U^\dagger(6)U^\dagger(2)\right] \\
&\quad \times [U(1)U(2)U(3)]_{\alpha'\beta'}\,|0\rangle, \\
&= 2\langle 0|U^\dagger_{\nu\alpha}(1)P_2(1)U_{\alpha'\tau}(1)\ \ U^\dagger_{\mu\nu}(2)U_{ab}(2)P_3(2)U^\dagger_{li}(2)U_{\tau\rho}(2) \\
&\quad \times\ \ U^\dagger_{\beta\mu}(3)P_2(3)U_{\rho\beta'}(3)\ \ U^\dagger_{df}(4)P_2(4)U_{jk}(4) \\
&\quad \times\ \ U^\dagger_{fa}(5)P_2(5)U_{ij}(5)\ \ U_{bd}(6)P_2(6)U^\dagger_{kl}(6)|0\rangle, \\
&= 2\ \tfrac{1}{2}\delta_{\nu\tau}\delta_{\alpha\alpha'}\ \tfrac{1}{12}\left(2\delta_{ai}\delta_{\nu\tau}-\delta_{\nu a}\delta_{i\tau}\right)\left(2\delta_{\mu\rho}\delta_{bl}-\delta_{\mu b}\delta_{l\rho}\right) \\
&\quad \tfrac{1}{2}\delta_{\beta\beta'}\delta_{\mu\rho}\ \ \tfrac{1}{2}\delta_{dk}\delta_{fj}\ \ \tfrac{1}{2}\delta_{fj}\delta_{ai}\ \ \tfrac{1}{2}\delta_{bl}\delta_{dk}, \\
&= \tfrac{3}{4}\delta_{\alpha\alpha'}\delta_{\beta\beta'}.
\end{aligned} \tag{47}
$$

Hence, the contribution from class (c) of intermediate states is $-3x^2/14$.

To calculate the contributions from class (d), we use the same labelling of links as for (b) and (c), but now we ignore link 1. Our starting state is now

$$|\Omega_{1;\alpha\beta}\rangle = \sqrt{2}\ U_{\alpha\beta}(3)|0\rangle, \tag{48}$$

and the zero-th order energy of the intermediate states is $(3/4)(L+4)$. Then,

$$
\begin{aligned}
\sum_{rs} |\langle d_{rs}|H_{\rm int}|\Omega_{1;\alpha\beta}\rangle|^2 &= \langle\Omega_{1;\alpha\beta}|H_{\rm int}\ P_2(2)P_2(3)P_2(4)P_2(5)P_2(6)\ H_{\rm int}|\Omega_{1;\alpha'\beta'}\rangle, \\
&= 2\langle 0|U^\dagger_{\beta\alpha}(3){\rm Tr}\left[U^\dagger(2)U(5)U(4)U^\dagger(6)\right]\ P_2(2)P_2(3) \\
&\quad \times P_2(4)P_2(5)P_2(6)\ {\rm Tr}\left[U(6)U^\dagger(4)U^\dagger(5)U(2)\right] U_{\alpha'\beta'}(3)|0\rangle, \\
&= 2\langle 0|U^\dagger_{ab}(2)P_2(2)U_{li}(2)\ \ U^\dagger_{\beta\alpha}(3)P_2(3)U_{\alpha'\beta'}(3) \\
&\quad \times\ U_{cd}(4)P_2(4)U^\dagger_{jk}(4)\ \ U_{bc}(5)P_2(5)U^\dagger_{kl}(5)\ \ U^\dagger_{da}(6)P_2(6)U_{ij}(6)|0\rangle, \\
&= 2\ \tfrac{1}{2}\delta_{ai}\delta_{bl}\ \tfrac{1}{2}\delta_{\beta\beta'}\delta_{\alpha\alpha'}\ \tfrac{1}{2}\delta_{ck}\delta_{dj}\ \tfrac{1}{2}\delta_{bl}\delta_{ck}\ \tfrac{1}{2}\delta_{dj}\delta_{ai}, \\
&= \delta_{\alpha\alpha'}\delta_{\beta\beta'}.
\end{aligned}
$$

Thus, the contribution to the energy is $-x^2/3$. Combining all contributions, we find

$$\mathcal{E}_{\overline{Q}Q} - \mathcal{E}_{\rm vac} = \left(\frac{3}{4} - \frac{2}{21}x^2\right) L. \tag{49}$$

Now we turn to the first several excited states. At zero-th order in perturbation theory, the first excited energy is

$$\mathcal{E}^{(0)}_{1,\overline{Q}Q} - \mathcal{E}^{(0)}_{\rm vac} = \frac{3}{4}(L+2). \tag{50}$$

This energy level is $L(L+1)$-fold degenerate. In other words, there are $L(L+1)$ states in which the quark and the antiquark are joined by a line of flux (in the fundamental representation) having length $(L+2)a$. In each of these states, the path of the flux joining the quark-antiquark pair is a straight line with a staple of width a. The staple can extend in either of the two transverse directions (we shall refer to these two directions as *left* or *right*) and can have any length from a to La. We shall refer to these states using the notation $|\Omega^{(d)}_{L+2}(x_1,x_2)\rangle$ where the superscript $d=r,l$ indicates the right or left direction of the staple, and x_1 and x_2 indicate the beginning and ending of the staple as measured from the start of the path.

To determine the energy levels at first-order in perturbation theory, we must diagonalize $H_{\rm int}$ within the $L(L+1)$-dimensional subspace spanned by the degenerate zero-th order strong-coupling states. To facilitate this, consider the following link labelling scheme shown below:

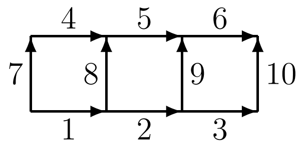

Now consider the following states (ignoring the colour sources at the ends):

$$\begin{aligned}
|\Omega^{(l)}_5(a,2a)\rangle &= \sqrt{2}\, U(1)U(8)U(5)U^\dagger(9)U(3)\ |0\rangle,\\
|\Omega^{(l)}_5(0,2a)\rangle &= \sqrt{2}\, U(7)U(4)U(5)U^\dagger(9)U(3)\ |0\rangle,\\
|\Omega^{(l)}_5(a,3a)\rangle &= \sqrt{2}\, U(1)U(8)U(5)U(6)U^\dagger(10)\ |0\rangle.
\end{aligned}$$

Now

$$\begin{aligned}
&\langle\Omega^{(l)}_5(0,2a)|\ H_{\rm int}\ |\Omega^{(l)}_5(a,2a)\rangle = 2\ \langle 0|\ \left[U^\dagger(3)U(9)U^\dagger(5)U^\dagger(4)U^\dagger(7)\right]_{\beta\alpha}\\
&\quad\times\ {\rm Tr}\left[U(7)U(4)U^\dagger(8)U^\dagger(1)\right]\ \left[U(1)U(8)U(5)U^\dagger(9)U(3)\right]_{\alpha'\beta'}\ |0\rangle,\\
&= 2\ \langle 0|\ U^\dagger_{li}(1)U_{\alpha' r}(1)\ U^\dagger_{\beta\mu}(3)U_{u\beta'}(3)\ U^\dagger_{\rho\tau}(4)U_{jk}(4)\ U^\dagger_{\nu\rho}(5)U_{st}(5)\\
&\quad\times\ U^\dagger_{\tau\alpha}(7)U_{ij}(7)\ U^\dagger_{kl}(8)U_{rs}(8)\ U_{\mu\nu}(9)U^\dagger_{tu}(9)\ |0\rangle,\\
&= 2\ \tfrac{1}{2}\delta_{lr}\delta_{\alpha' i}\ \tfrac{1}{2}\delta_{\beta\beta'}\delta_{u\mu}\ \tfrac{1}{2}\delta_{\rho k}\delta_{j\tau}\ \tfrac{1}{2}\delta_{\nu t}\delta_{s\rho}\ \tfrac{1}{2}\delta_{\tau j}\delta_{i\alpha}\ \tfrac{1}{2}\delta_{ks}\delta_{rl}\ \tfrac{1}{2}\delta_{\mu u}\delta_{t\nu},\\
&= \tfrac{1}{2}\delta_{\alpha\alpha'}\delta_{\beta\beta'}.
\end{aligned} \tag{51}$$

Similarly for $|\Omega^{(l)}_5(a,3a)\rangle$. Hence, we find

$$\begin{aligned}
\langle\Omega^{(d)}_{L+2}(x_1,x_2)|\ H_{\rm int}\ |\Omega^{(d')}_{L+2}(x_1',x_2')\rangle &= \frac{1}{2}\ \delta_{dd'}\ \Big[\delta_{x_1x_1'}\left(\delta_{x_2,x_2'-a}+\delta_{x_2,x_2'+a}\right)\\
&\quad+\delta_{x_2x_2'}\left(\delta_{x_1,x_1'-a}+\delta_{x_1,x_1'+a}\right)\Big].
\end{aligned} \tag{52}$$

This is the matrix to be diagonalized. For small L, the easiest way to proceed is by brute-force diagonalization. Results for $L=3$ and $L=4$ are given in Tables 10 and 11. We again label states which are symmetric (antisymmetric) under reflections in the molecular axis by S (A) and add the subscript g and u for states which are symmetric and antisymmetric, respectively, under the combined operations of charge conjugation and spatial inversion about the midpoint between the quark and the antiquark.

Table 10: Low-lying energy spectrum for $L = 3$. Energies in terms of the lattice spacing a_s are obtained by multiplying the results below by $g^2/8$. Note that $x = 4/g^4$ and $\beta = 4/g^2$. Thus, in terms of β, the results below must be multiplied by $1/(2\beta)$ and $x = \beta^2/4$.

S_g	$9 - \frac{8}{7}\, x^2$
S'_g, A_u	$15 - 2\sqrt{5}\, x$
S_u, A_g	$15 - 2\, x$
S''_g, S'''_g, A'_u, A''_u	15
S'_u, A'_g	$15 + 2\, x$
S''''_g, A'''_u	$15 + 2\sqrt{5}\, x$

Table 11: Low-lying energy spectrum for $L = 4$. Energies in terms of the lattice spacing a_s are obtained by multiplying the results below by $g^2/4$. Note that $x = 4/g^4$ and $\beta = 4/g^2$. Thus, in terms of β, the results below must be multiplied by $1/\beta$ and $x = \beta^2/4$.

S_g	$6 - \frac{16}{21}\, x^2$
S'_g, A_u	$9 - \left(1 + \sqrt{3}\right)\, x$
S_u, A_g	$9 - \sqrt{3}\, x$
S''_g, A'_u	$9 - x$
S'''_g, A''_u	$9 - \left(1 - \sqrt{3}\right)\, x$
S'_u S''_u, A'_g, A''_g	9
S''''_g, A'''_u	$9 + \left(1 - \sqrt{3}\right)\, x$
$S^{(5)}_g$, A''''_u	$9 + x$
S'''_u, A'''_g	$9 + \sqrt{3}\, x$
$S^{(6)}_g$, $A^{(5)}_u$	$9 + \left(1 + \sqrt{3}\right)\, x$

3 Comparison of results

The spectra for $R = 3$ and $R = 4$ calculated using the Monte Carlo method are compared to the expectations from strong-coupling theory in Figs. 1-4. Energies are shown in terms of a_s^{-1}, the inverse spatial lattice spacing. The results are in excellent agreement.

References

[1] M. Creutz, Phys. Rev. D **15**, 1128 (1977).

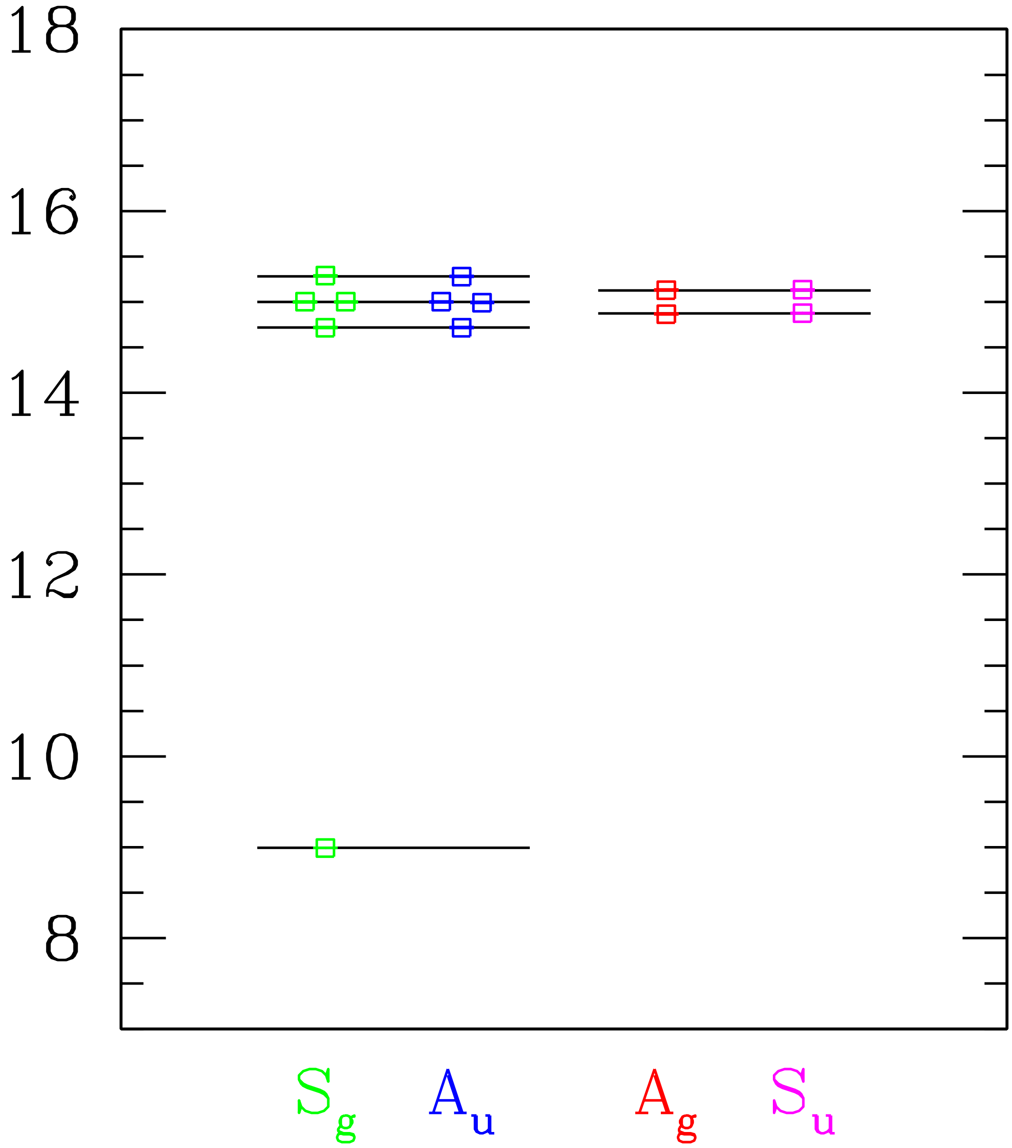

Figure 1: Comparison of the spectrum calculated using the Monte Carlo method (open squares) with the expectations from strong-coupling perturbation theory (the horizontal lines). The energies shown are in terms of a_s^{-1}, the inverse spatial lattice spacing, for $R = 3$ and $\beta = 0.5$ in the Hamiltonian limit.

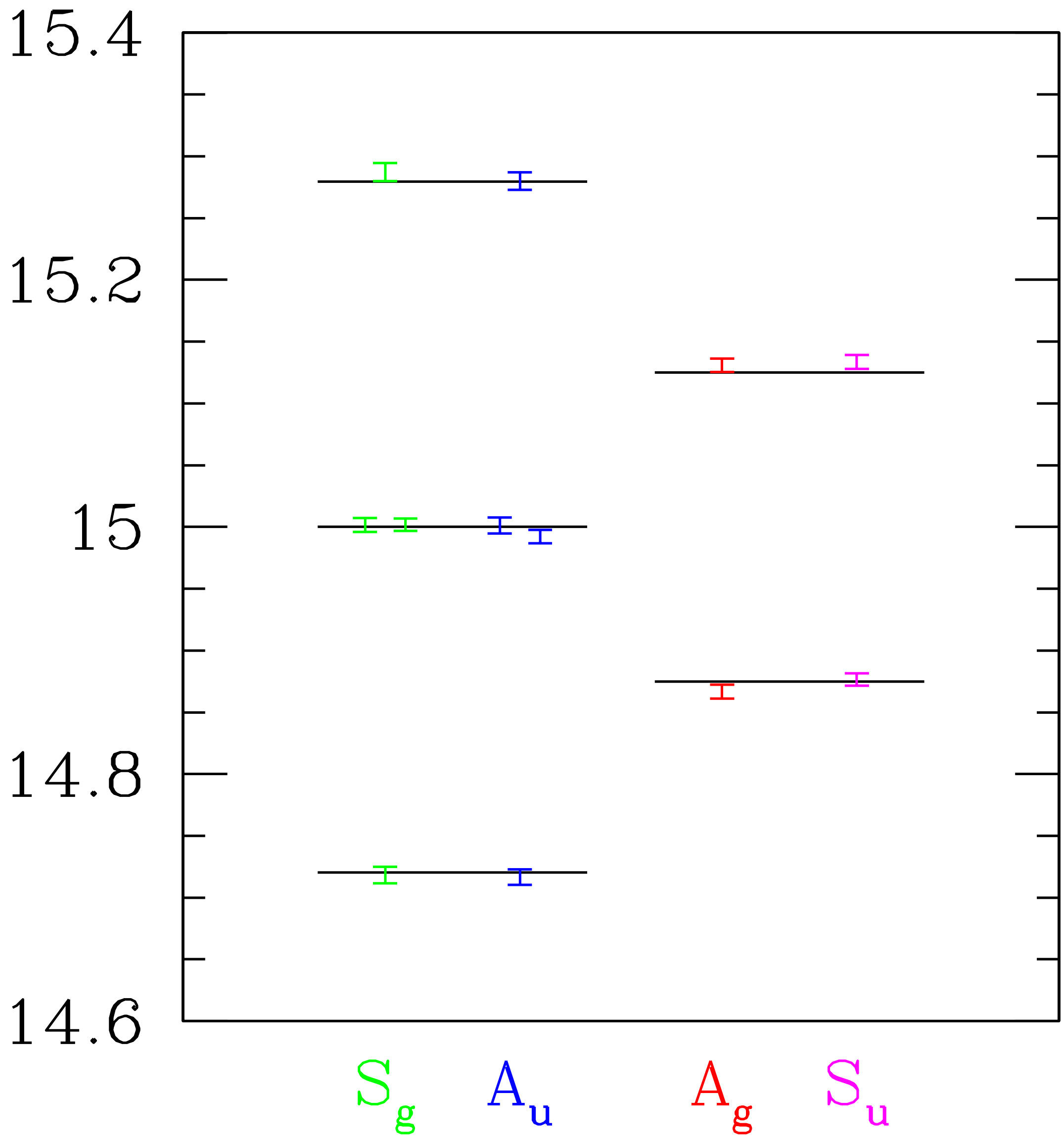

Figure 2: Comparison of the spectrum calculated using the Monte Carlo method (the error bars) with the expectations from strong-coupling perturbation theory (the horizontal lines). The energies shown are in terms of a_s^{-1}, the inverse spatial lattice spacing, for $R = 3$ and $\beta = 0.5$ in the Hamiltonian limit. This is a close-up of the first band lying above the ground state.

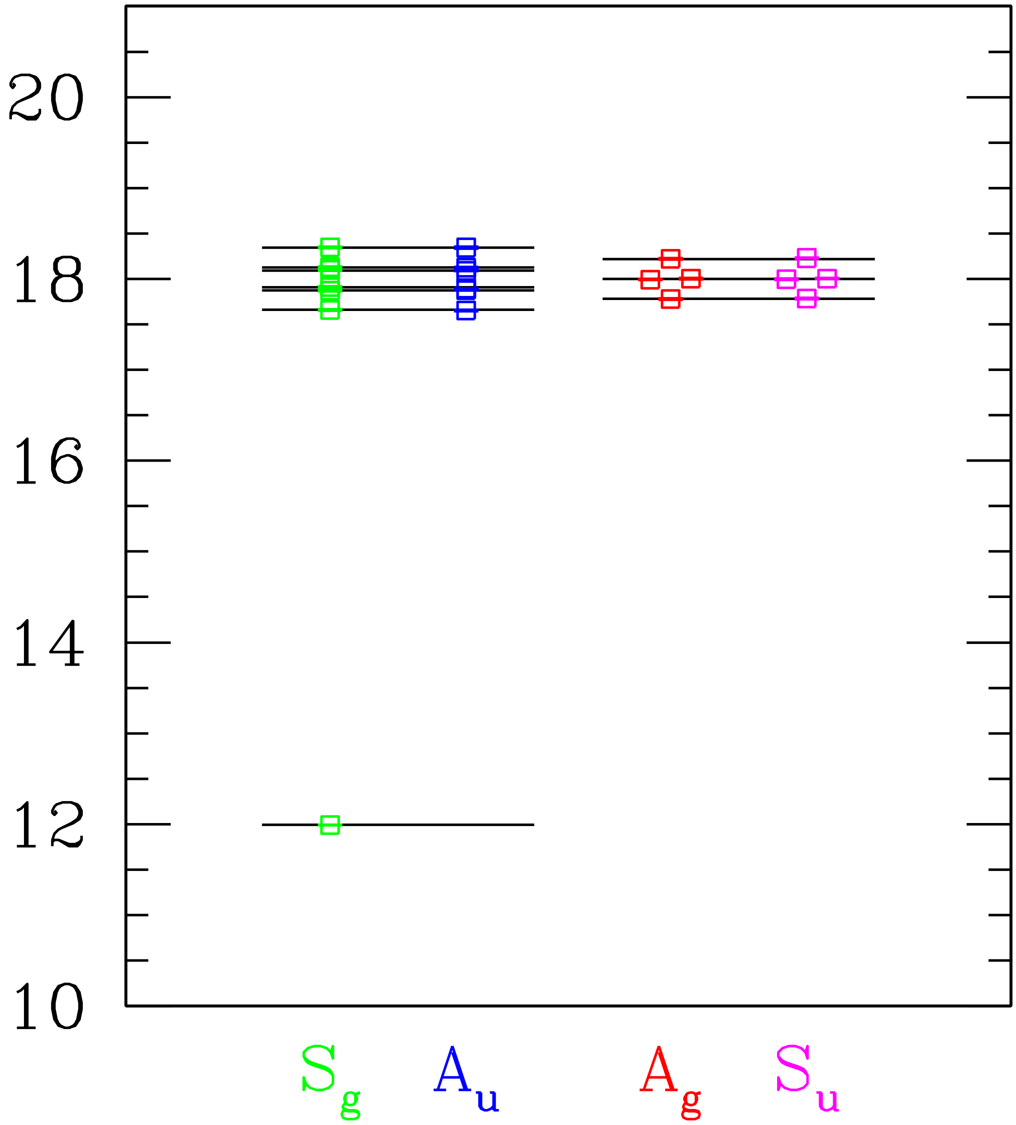

Figure 3: Comparison of the spectrum calculated using the Monte Carlo method (open squares) with the expectations from strong-coupling perturbation theory (the horizontal lines). The energies shown are in terms of a_s^{-1}, the inverse spatial lattice spacing, for $R = 4$ and $\beta = 0.5$ in the Hamiltonian limit.

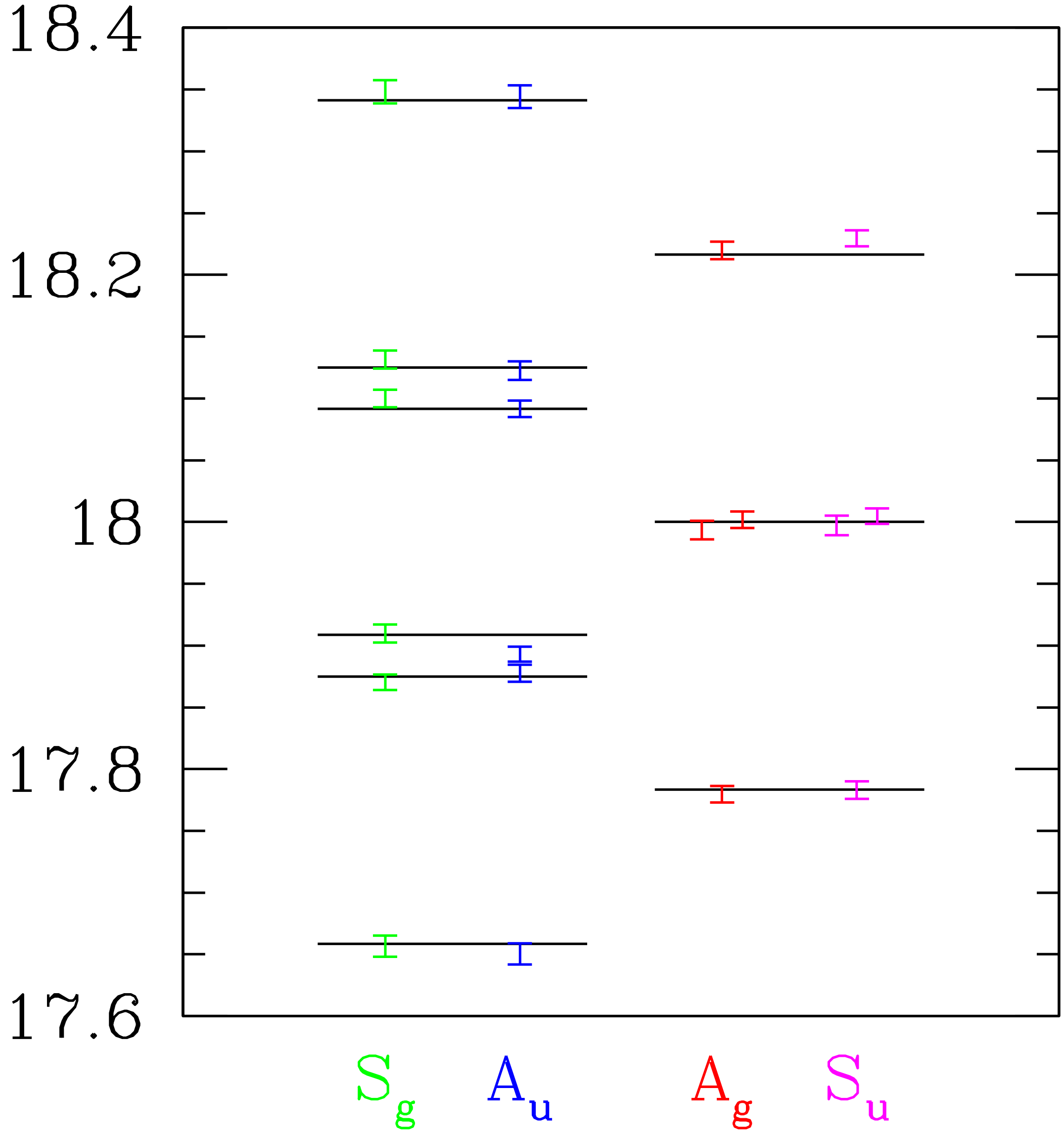

Figure 4: Comparison of the spectrum calculated using the Monte Carlo method (the error bars) with the expectations from strong-coupling perturbation theory (the horizontal lines). The energies shown are in terms of a_s^{-1}, the inverse spatial lattice spacing, for $R = 4$ and $\beta = 0.5$ in the Hamiltonian limit. This is a close-up of the first band lying above the ground state.